




Research Article



Thermal Effect on The Post-buckling And Mechanical Response of Single-Walled Carbon Nanotubes: A Numerical Investigation

Sima Besharat Ferdosi* *Department of Mechanical Engineering, Lamar University, Beaumont, TX, 77710, USA*

Keywords

Carbon nanotubes,
Buckling,
Post-buckling,
Imperfection,
Thermal Analysis,
Numerical simulation,
Structural mechanics.

Abstract

The subject of this article is the study of the post-buckling behavior of single-walled carbon nanotubes (SWCNT) under various thermal conditions, different lengths, and chiralities. The critical buckling loads should be found first to investigate the post-buckling behavior. Then the buckling modes are used as a geometrical imperfection to analyze the post-buckling path. For post-buckling analysis, the boundary conditions are assumed to be clamped. A space-frame model is here employed for the zigzag and armchair nanotubes with different chiralities and aspect ratios. This approach models the linkage between carbon atoms as a three-dimensional elastic beam. The sectional property parameters of these beam members are obtained by establishing a linkage between structural and molecular mechanics. This strategy is far more affordable and faster than the molecular dynamics simulation technology approach, which was previously used. The obtained results indicate that, as expected, the critical buckling load decreases by increasing the aspect ratio of the nanotubes as well as chirality. Also, it is noticed that the post-buckling behavior of both armchair and zigzag nanotubes are quite similar. In addition, the effect of temperature on the post-buckling behavior is investigated. Due to the influence of temperature over the linkage length and force field constants it is shown that when the temperature increases a decline in the critical buckling loads is observed and the post-buckling path also goes through this decreasing process. It is the same for both nanotubes.

1. Introduction

By finding the carbon nanotubes, hereinafter CNTs, in 1991 by Iijima [1], new windows of science have been opened to mankind due to the CNTs' exceptional different potential applications in nanocomposites, nanoelectronics, nanosensors, and nanofilms. Nanotubes have superior attributes mechanical, electrical, and thermal properties. Especially their unique geometry and mechanical properties have made them have many practical applications in the industry [2]. The need to comprehend and regulate nanomaterials' physical and mechanical behaviors has grown over the past decades, with a substantial interest in their

applications in different fields. For example, many studies have reported the presence of nano additives in the base fluid improves heat transfer performance. Sharifat et al. examined the heat transfer coefficient of water in a heat exchanger system after adding Al₂O₃ nanoparticles and showed superior cooling performance in the presence of nano additives [3,4]. In 2022, Ferdosi et al [5], studied the single-walled carbon nanotubes' elastic modulus by using the asymptotic homogenization method. They used the asymptotic homogenization method to investigate the mechanical characteristics of single-walled carbon nanotubes. Young's modulus and shear modulus have been estimated for both armchair and zigzag nanotubes in

* Corresponding Author: Sima Besharat Ferdosi

E-mail address: sbesharatfer@lamar.edu, ORCID: <https://orcid.org/0009-0008-3783-1939>

Received: 10 April 2023; Revised: 18 April 2023; Accepted: 20 April 2023

<https://doi.org/10.61186/crpase.9.2.2845>

Academic Editor: **He Li**

Please cite this article as: S. Besharat Ferdosi, Thermal Effect on The Post-buckling And Mechanical Response of Single-Walled Carbon Nanotubes: A Numerical Investigation, Computational Research Progress in Applied Science & Engineering, CRPASE: Transactions of Mechanical Engineering 9 (2023) 1–6, Article ID: 2845.

accordance with the relationships between the derived coefficients and molecular mechanical characteristics. Investigations have been done into how diameter and orientation affect the mechanical characteristics of carbon nanotubes.

One of the most important issues raised in the discussion of nanotubes is the buckling and stability of carbon nanotubes against various forces. In 2005, Yu Wang & Xiu Wang conducted studies on the compressive deformation of single-walled carbon nanotubes using the molecular dynamics simulation method [6]. To investigate the buckling behavior of single-walled carbon nanotubes under various boundary conditions, Ansari and Rouhi [7] created an atomistic finite element model. The elastic moduli of the beam elements are found through a connection between molecular mechanics and structural mechanics. Additionally, the behavior of armchair and zigzag nanotubes under buckling loads was examined depending on the L/D aspect ratio. In 2006, Zhang and Shen studied the buckling and post-buckling behavior of armchair and zigzag single-walled carbon nanotubes under axial compressive load, torsion, and compression [8]. They used the molecular dynamics simulation technique and based their findings on the solution of the Lennard-Jones potential function. They studied how temperature changes and van der Waals forces affected buckling and concluded that van der Waals forces have no impact on how single-walled carbon nanotubes buckle under axial compressive load. Mehdi Eftekhari et al, in 2013, The molecular dynamics method has been used to study the local buckling behavior of perfect/defective and single/multi-walled carbon nanotubes (CNTs) under axial compressive forces [9]. The findings demonstrate that while defects have little impact on a CNT's compressive elastic modulus, they significantly lower buckling stress and the ratio of an immediate reduction in buckling compressive stress of the defective CNT to the perfect one. N. Mohamed et al [10], in 2022, studied Buckling and post-buckling behaviors of higher-order carbon nanotubes using the energy-equivalent model. They Utilize an energy-equivalent model and examine the impact of size scale on the buckling and post-buckling of single-walled carbon nanotubes (SWCNTs) supported by nonlinear elastic supports. In 2022, Alessandra Genoese et al [11] investigated buckling and post-buckling analysis of single-wall carbon nanotubes using molecular mechanics. To examine the effectiveness of the model and the function of the quaternary interactions in contexts of both global and local behaviors, several case studies involving zigzag and armchair tubes of various aspect ratios, under compression, bending, and torsion, are addressed.

2. Finite Element Modeling of SWCNTs

The concept of molecule structural mechanics was motivated by the geometric resemblance between macroscopic frame structures and nanoscale fullerenes [7]. In fact, the behavior of SWCNTs, which are thought of as space-frame structures, can be described using techniques from classical physics. This is done using a 3-D finite element model with beam elements for the bonds and focused masses for the carbon atoms. The elastic properties

of these beams are controlled by the interaction between structural mechanics and molecular mechanics.

The steric potential energy, which is connected to the spatial arrangement of atoms in a molecule and in particular affects chemical reactions, can also be used to determine the force field. The amount of energy is determined by the respective positions of the nuclei that make up the carbon molecule. Eq. (1) is a general formulation of the complete steric potential energy of an SWNT under modest strain while ignoring the electrostatic interactions. It contains the sum of energies due to the valence of bonded iterations of bonded and non-bonded contacts [12].

$$U_{tot} = \sum U_r + \sum U_\theta + \sum U_\phi + \sum U_\omega + \sum U_{vdw} \quad (1)$$

Where the U s are energies associated with:

$$U_r = (1/2)k_r(r - r_0)^2 = (1/2)k_r(\Delta r)^2 \quad (2)$$

$$U_\theta = (1/2)k_\theta(\theta - \theta_0)^2 = (1/2)k_\theta(\Delta\theta)^2 \quad (3)$$

$$U_\tau = U_\phi + U_\omega = (1/2)k_\tau(\Delta\phi)^2 \quad (4)$$

In Eqs. (2-4) k_r, k_θ & k_τ correspond to the force constants associated with the stretching, bending, and torsion of bonds, and $\Delta r, \Delta\theta$ & $\Delta\phi$ denote the deviation of bond length, bond angle and dihedral angle from the equilibrium position, respectively.

Elastic beams with the young's modulus E , length L , and cross-sectional area A , are taken as the elements representing the bond.

The strain energy under pure tension N is given by:

$$U_A = \frac{1}{2} \int_0^L \frac{N^2}{EA} dl = \frac{1}{2} \frac{N^2}{EA} = \frac{1}{2} \frac{EA}{L} (\Delta L)^2 \quad (5)$$

The strain energy of the beam element under pure bending moment M is:

$$U_M = \frac{1}{2} \int_0^L \frac{M^2}{EI} dl = \frac{1}{2} \frac{EI}{L} \alpha^2 = \frac{1}{2} \frac{EI}{L} (2\alpha)^2 \quad (6)$$

The strain energy of the beam element under pure twisting moment T is given by:

$$U_T = \frac{1}{2} \int_0^L \frac{T^2}{GJ} dl = \frac{1}{2} \frac{T^2 L}{GJ} = \frac{1}{2} \frac{GJ}{L} (\Delta\beta)^2 \quad (7)$$

Given that Eqs. (2-4) and (5-7), which represent the potential energy terms in the molecular and structural systems, respectively, are similar, the parameters of structural mechanics can be related to those of molecular mechanics as follows:

$$\frac{EA}{L} = k_r, \quad \frac{EI}{L} = k_\theta, \quad \frac{GJ}{L} = k_\tau \quad (8)$$

The elastic properties of the isotropic beam components with diameter d and length L can therefore be determined using Eq. (9).

$$d = 4 \sqrt{\frac{k_\theta}{k_r}}, \quad E = \frac{k_r^2 L}{4\pi k_\theta}, \quad G = \frac{k_r^2 k_\tau L}{8\pi k_\theta^2} \quad (9)$$

Table 1. The parameters used in the FEM model [13].

$k_r \left(\frac{N}{nm}\right)$	$k_\theta \left(\frac{Nnm}{rad^2}\right)$	$k_\tau \left(\frac{Nnm}{rad^2}\right)$	$d(\text{\AA})$	$E \left(\frac{N}{\text{\AA}^2}\right)$	$G \left(\frac{N}{\text{\AA}^2}\right)$
6.52×10^{-7}	8.76×10^{-10}	2.78×10^{-10}	1.466	5.488×10^{-8}	8.701×10^{-9}

3. Temperature Effect on Constant Force Filed

The potential energy of a molecular arrangement is determined using Eq. (1). We could disregard all terms in place of the first two terms to analyze SWCNT under axial load at all temperatures. Eq (1) could then be presented in a different way using Eq (10) as an outcome.

$$U_{tot} = \sum U_r + \sum U_\theta \quad (10)$$

In other words, the distance between two atoms increases with rising temperature and vice versa in SWCNT under axial loading in the remaining 120 degrees. Eq (11) is used to determine changing length:

$$\alpha_T = \alpha(1 + \alpha T) \quad (11)$$

In above equation, T is temperature and α is the thermal expansion coefficient, the is calculated in all ranges of temperature [12].

Tensile force constant K_r^T and bending angel K_θ^T are calculated from badger's equation as follows [14]:

$$K_r^T = \frac{1}{(1 + \alpha T)^3} K_r \quad (12)$$

$$K_\theta^T = \frac{1}{(1 + \alpha T)^3} K_\theta \quad (13)$$

4. Investigating the Post-buckling Behavior of Carbon Nanotubes at Ambient Temperature

As space-frame structures, SWCNTs are modeled as an atomistic finite element system with beam components using the Abaqus FE code. The connections are simulated by the elastic three-dimensional B4 element. It has six degrees of freedom at each node, which can be used to rotate around the x, y, and z axes as well as translate in the x, y, and z dimensions. To model the post-buckling phenomenon in the Abaqus software, we first compute the critical buckling loads as well as buckling modes. Then, the location changes of the nodes, induced by the buckling modes, are considered as a geometry imperfection to derive the post-buckling path. It should be noted that the software's geometric nonlinear analysis mode is used to conduct post-buckling analysis. The user must establish the link between the two components, buckling, and post-buckling, because they are not present in

The parameters that are supplied to the FE model as inputs for the beam elements are enumerated in Table 1 and are based on the covalent bond distance of the carbon atoms in the hexagonal lattice, which is 0.142 nm.

the software's default working environment, it is further stated. To evaluate the post-buckling behavior in this case, Ferdosi et al.'s investigations' results for critical buckling loads and buckling modes are used [13]. They hired the space-frame model to investigate the critical buckling loads and buckling modes on different boundary conditions, chiralities, and temperatures.

An SWCNT's geometry can be described in terms of its radius R , nanotube length L , and nanotube chirality determined by unit vector values (n,m) . Since armchair SWCNT dimensions don't always meet zigzag ones, the closets are practical. In this part, we examine the impact of variables like chirality and length on the nonlinear post-buckling phenomenon at a 27 °C ambient temperature. Armchair nanotubes (12,12), with $R=8.13 \text{ \AA}$, & $L=112 \text{ \AA}$, and zigzag nanotubes (21,0) with $R=8.22 \text{ \AA}$, & $L=113.7 \text{ \AA}$ are studied under the axial displacement. Figures (1) and (2), for clamped supported boundary conditions, demonstrate reasonable agreements between the results of the current study and Zhang's [8] research.

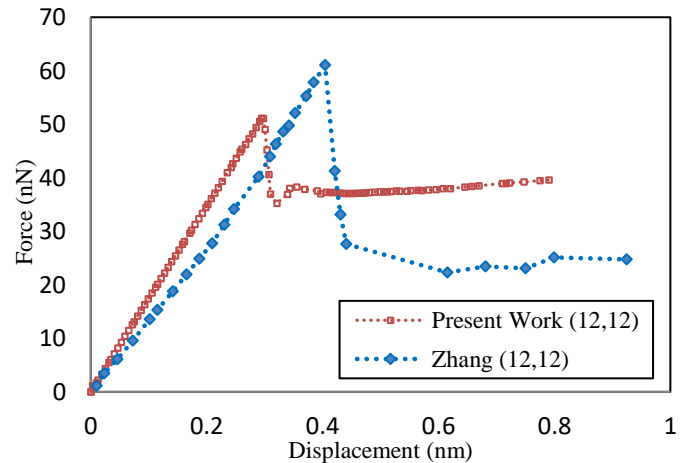


Figure 1. Comparison of post-buckling path zigzag (12,12) between Zhang's and Present Work results

Figure 3 shows the force expressed versus displacement that illustrates the effects of chirality on the direction of carbon nanotubes' post-buckling path. It demonstrates how the graphs steadily move in an upward direction until they reach the critical buckling load. Then, a sudden sharp decrease in force happens as soon as the displacement slightly increases. After that, the nanotubes enter the post-buckling nonlinear area. With increasing displacement

following a sudden decrease in force, the quantity of force changes is minimal and can be ignored. It is demonstrated that post-buckling paths are almost the same for nanotubes with various chiralities.

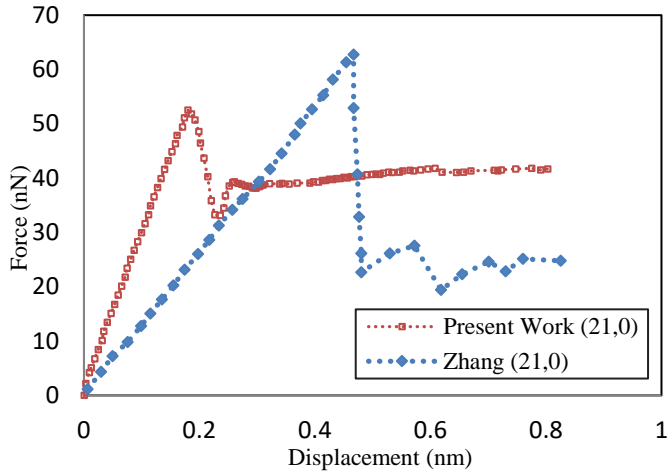


Figure 2. Comparison of post-buckling path armchair (21,0) between Zhang's and Present Work results

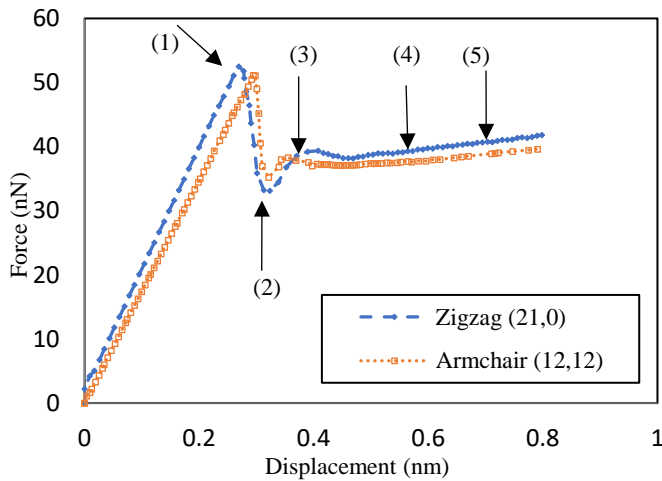


Figure 3. Effect of chirality on the post-buckling behavior of armchair (12,12) and zigzag (21,0) nanotubes with clamped boundary condition

Figure 4 shows the deformations caused by buckling for the armchair nanotube (12,12) with a length of 11.2 nm for the clamped boundary condition. Mode (1) is the starting point of buckling, which occurs at a displacement of 0.294 nm. The deformation shown in mode (2) corresponds to the minimum point of the diagram in the post-buckling part. This point represents the lowest amount of force after the buckling stage, which occurs at a displacement of 0.321 nm. Modes (3), (4), and (5) respectively represent deformation in displacements of 0.437 nm, 0.657 nm, and 0.803 nm in the horizontal part of the post-buckling diagram.

The positions of the mentioned modes are shown in the corresponding load-displacement diagram. At shortenings and curvatures, many local deformations are observed in the nanotube structure. It can be seen carefully in the deformed beam elements (which can be seen by magnifying the deformed structure) that these shapes are caused by the

elastic deformations of the beams and no entanglement is observed in the beam. The obtained results are in significant agreement with the molecular dynamics simulations reported in references [8,15], which proves the validity of the structural mechanic method used in this method. In other words, the geometry and forces extracted from the potential functions used in this paper are close to reality.

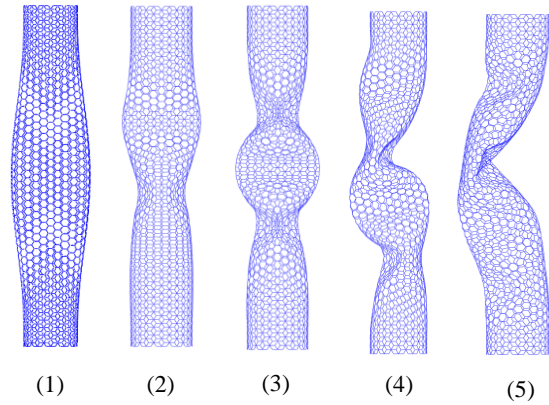


Figure 4. Configurations of deformation caused by buckling for the armchair nanotube (12,12) by applying axial displacement for the clamped boundary condition.

After observing the effect of chirality on the post-buckling behavior, we investigate the effect of length on it. For this purpose, post-buckling analysis was performed for armchair nanotubes (12,12) with lengths of 7.26 nm, 11.2 nm, and 14.64 nm and zigzag nanotubes (21,0) with lengths of 7.105 nm, 10.7 nm, 11.37 nm, and 14.35 nm under the clamped boundary conditions. (Figures 5 and 6). It shows that with the increase in length, the final buckling load decreases. Also, with the increase in length, the final buckling load of nanotubes occurs at a larger displacement. The reason for this is that the occurrence of instability in a nanotube with a longer length requires more displacement. By comparing Figures 5 and 6 for armchair and zigzag nanotubes, we conclude that the effect of length on both nanotubes is the same.

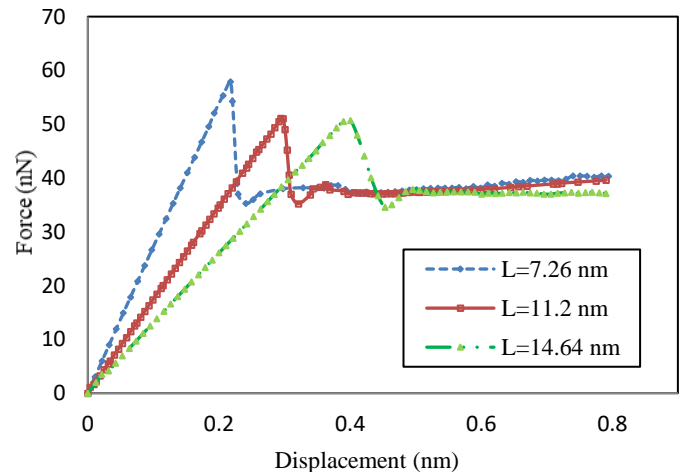


Figure 5. The effect of length on the armchair nanotube (12,12) with clamped boundary condition

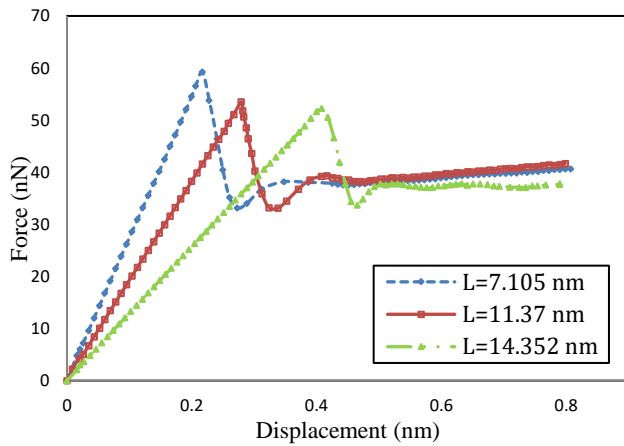


Figure 6. The effect of length on the zigzag nanotube (21,0) with clamped boundary condition

5. The Effect of Temperature Changes on the Post-Buckling Behavior of Carbon Nanotubes

We have examined the post-buckling path at temperatures of -173, 27, and 527 Celsius to find out how temperature affects the post-buckling behavior of armchair and zigzag nanotubes. As shown in Figures 7 and 8, the critical buckling load reduces as the temperature rises from -173 to 527 degrees Celsius, and the post-buckling path also undergoes this decreasing process. It applies to both nanotubes equally.

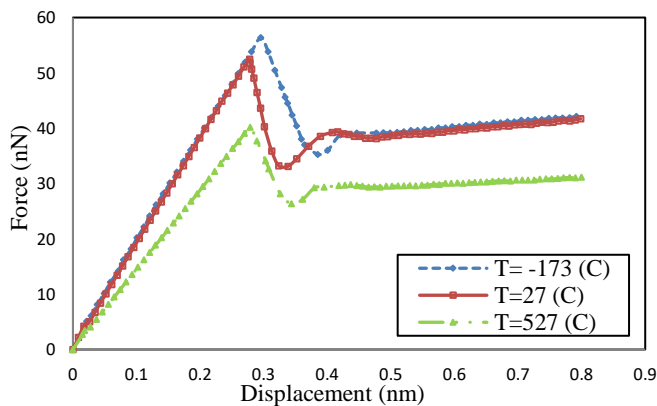


Figure 7. The effect of temperature on the zigzag nanotube (21,0) with clamped boundary condition

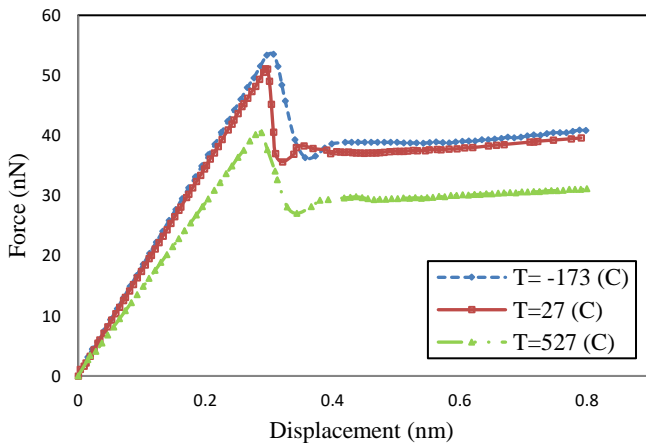


Figure 8. The effect of temperature on the armchair nanotube (12,12) with clamped boundary condition

6. Conclusion

Nanotube post-buckling refers to the behavior of carbon nanotubes when they are subjected to compressive loads that cause them to buckle, and then continue to deform in a nonlinear way. Investigation of this phenomenon is significant because of its potential for developing new materials, devices, and technologies that could revolutionize various fields, including electronics, energy, and medicine. The ability of carbon nanotubes to demonstrate an outstanding degree of mechanical resilience against the compressive force is one of this article's significant achievements. Computational simulations have been used to study the post-buckling behavior of carbon nanotubes. These simulations are considerably faster and less costly than experimental investigations, but they also have good agreement with them. The obtained results demonstrate that, as expected, the critical buckling load decreased about 15% by increasing the length to approximately two times. Additionally, it has been observed that as length increases, the final buckling load happens at a larger displacement for nanotubes with longer lengths. Furthermore, by analyzing the impact of temperature on the post-buckling path of carbon nanotubes, we draw the conclusion that the critical buckling load reduces near 28% with increasing temperature from -173 to 527 Celsius. This decreasing process, which is the same for zigzag and armchair nanotubes, also occurs on the route of buckling.

References

- [1] S. Iijima, Helical microtubules of graphitic carbon, *Nature* 354 (1991).
- [2] P. G. Kumar, Application of Nano Silica to Improve Self-Healing of Bitumen Mixtures, *Computational Research Progress in Applied Science and Engineering*, 06 (2022) 276–280.
- [3] F. Sharifat, A. Marchitto, M. S. Solari, D. Toghraie, D. Toghraie, Analysis, prediction, and optimization of heat transfer coefficient and friction factor of water-Al₂O₃ nanofluid flow in shell-and-tube heat exchanger with helical baffles (using RSM), *European Physical Journal Plus* 137 (2022).
- [4] M. Derikvand, M. S. Solari, D. Toghraei, Entropy generation and forced convection analysis of ethylene glycol/MWCNTs-Fe₃O₄ non-Newtonian nanofluid in a wavy microchannel with hydrophobic surfaces, *Journal of the Taiwan institute of chemical engineers* 143 (2023).
- [5] S. B. Ferdosi, M. Porbashiri, Calculation of the Single-Walled Carbon Nanotubes' Elastic Modulus by Using the Asymptotic Homogenization Method, *International Journal of Science and Engineering Applications* 11 (2022) 254–265.
- [6] Y. Wang, X. Wang, Simulation of the elastic response and the buckling modes of single walled carbon nanotubes. *Materials Science* 32 (2005) 141–146.
- [7] R. Ansari, S. Rouhi, Atomistic finite element model for axial buckling of single-walled carbon nanotubes, *Physica E43* (2010) 58–69.
- [8] C. L. Zhang, H. S. Shen, Buckling and postbuckling analysis of single-walled carbon nanotubes in thermal environments via molecular dynamics simulation, *Carbon* 44 (2006) 2608–2616.
- [9] M. Eftekhari, S. Mohammadi, A. Khoei, Effect of defects on the local shell buckling and post-buckling behavior of single and multi-walled carbon nanotubes, *Computational Materials Science* 79 (2013) 736–744.

- [10] N. Mohamed, S. A. Mohamed, M. A. Eltaher, Buckling and post-buckling behaviors of higher order carbon nanotubes using energy-equivalent model, *Engineering with Computers* 37 (2021) 2823–2836.
- [11] A. Genoese, G. Salerno, Buckling and post-buckling analysis of single wall carbon nanotubes using molecular mechanics, *Applied Mathematical Modelling* 83 (2020) 777–800.
- [12] A. K. Rappe, C. J. Casewit, K. S. Colwell, Application of a universal force field to organic molecules, *Journal of American Chemical Society* 114 (1992).
- [13] S. B. Ferdosi, N. Mohammadyahya, M. Abbasi, Axial Buckling of Single-walled Nanotubes Simulated by an Atomistic Finite Element Model under Different Temperatures and Boundary Conditions, *International Journal of Science and Engineering Applications* 11 (2022) 151–163.
- [14] X. Guo, J. B. Wang, H. W. Zhang, Mechanical properties of single-walled carbon nanotubes based on higher order Cauchy-Born rule, *International Journal of Solids and Structures* 43 (2006) 1276–1290.
- [15] N. Silvestre, B. Faria, A molecular dynamics study on the thickness and post-critical strength of carbon nanotubes, *Composite Structure* 94 (2012) 1352–1358.